ISSN 0010-9525, Cosmic Research, 2014, Vol. 52, No. 5, pp. 342–352. © Pleiades Publishing, Ltd., 2014.
Original Russian Text © M.V. Zakhvatkin, Yu.N. Ponomarev, V.A. Stepan'yants, A.G. Tuchin, G.S. Zaslavskiy, 2014, published in Kosmicheskie Issledovaniya, 2014, Vol. 52, No. 5, pp. 376–386.

Navigation Support for the RadioAstron Mission

M. V. Zakhvatkin[a], Yu. N. Ponomarev[b], V. A. Stepan'yants[a], A. G. Tuchin[a], and G. S. Zaslavskiy[a]

[a] *Keldysh Institute of Applied Mathematics, Russian Academy of Sciences, Miusskaya pl. 4, Moscow, Moscow, 125047 Russia*
e-mail: zakhvatkin@kiam1.rssi.ru

[b] *Astro Space Center of Lebedev Physical Institute, Russian Academy of Sciences, Moscow, Russia*

Received December 16, 2013

Abstract—A developed method of determination of orbital parameters allows one to estimate, along with orbit elements, some additional parameters that characterize solar radiation pressure and perturbing accelerations due to unloadings of reactiion wheels. A parameterized model of perturbing action of solar radiation pressure on the spacecraft motion is described (this model takes into account the shape, reflecting properties of surfaces, and spacecraft attitude). Some orbit determination results are presented obtained by the joint processing of radio measurements of slant range and Doppler, laser range measurements used to calibrate the radio measurements, optical observations of right ascension and declination, and telemetry data on spacecraft thrusters' firings during an unloading of reaction wheels.

DOI: 10.1134/S0010952514050128

ACCURACY REQUIREMENTS OF SPACECRAFT MOTION PARAMETERS DETERMINATION

Astronomical observations with the space radio telescope (SRT),[1] along with ground-based radio telescopes (GRTs), combined in a radio interferometer allow one to study radio sources with much better angular resolution than provided by terrestrial VLBI [1, 2]. Necessary data on the angular position of details of observed radio source are implicitly contained in the value of geometric delay τ of arrival of its wave front at the interferometer's antennas.

Figure 1 shows two radio telescopes that represent parts of a radio interferometer; one of them is located on the Earth and the other is in the satellite's orbit. Both of the radio telescopes observe the same source simultaneously. The vector $\mathbf{b} = \mathbf{r}_2 - \mathbf{r}_1$ is referred to as base vector.

The delay τ can be obtained using correlation analysis of signals from two telescopes. A radio signal received by the space radio telescope is amplified by a low-noise amplifier, then isolated using an appropriate filter and its spectrum is coherently transferred to intermediate frequency (IF) (496–528) MHz. Omitting details, we say that, later, the spectrum of IF signal is transferred to the video region $(0–\Delta f_k)$. Then, the signal is limited at the zero level (clipping operation), quantized with a time step $\Delta t_k = 1/(2\Delta f_k)$, and transformed into a stream of digital data that is then transmitted in the direct transmission mode to the tracking station (TS). The bandwidth of recording for the RadioAstron mission is $f_k = 32$ MHz.

In the ideal case, when signals are sampled with a step of Δt_k, and one-bit quantization of radio signal is used, there would be two identical bit streams at the outputs of two radio telescopes shifted by a value of delay τ of signal front arrival to these telescopes. Since the relative positions, velocities, and accelerations of the SRT and GRT vary with time, phase and frequency shifts are variable, and one should compensate for them in correlation processing. In other words, to

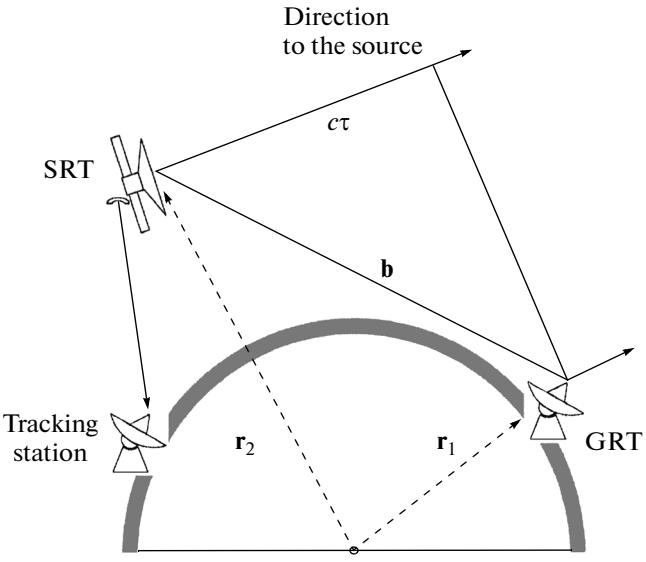

Fig. 1. Scheme of operation of ground–space interferometer.

[1] Technical characteristic of the SRT, as well as the latest news on the project status, can be found at the website http://www.asc.rssi.ru/radioastron/index.html.

calculate the cross correlation function, data streams from the SRT and GRT should be coordinated in time and frequency. The time mismatch or delay arise due to the nonsimultaneous arrivals of the wave front at telescope antennas, while disparities originate in the frequencies due to the Doppler shift of the frequency at a relative velocity of motion of the antennas along the direction to a radio source.

We assume that the plane wave front of a monochromatic signal first reaches GRT at moment t_1, then arrives at SRT at the moment $t_2 = t_1 + \tau$. Hence,

$$c\tau = c(t_2 - t_1) = -\mathbf{b}\cdot\mathbf{s} = -(\mathbf{r}_2 - \mathbf{r}_1)\cdot\mathbf{s}, \quad (1)$$

where c is the velocity of light.

For the correlation processing of the data of a ground–space interferometer, one must know the interferometer base $\mathbf{b}$ with high precision at every moment. This base is determined both by the position of the ground-based radio telescope and by the position of the SRT. For the correlation processing of the observation data of weak radio sources, it is required to accumulate the signal coherently over an interval of tens or even hundreds of seconds. For this purpose, one should know with high accuracy not only the velocities, but also the SRT acceleration. Admissible error in position is determined by the technical parameters of the correlator (number of channels) and by the interval of onboard signal discretization, while admissible errors in velocity and acceleration are determined by the moment of misalignment. For example, if, at relative radial velocity of the telescopes of $V = 3$ km/s, the clock frequency of bit stream f_k attains the Doppler increment

$$\delta f_k = f_k \frac{V}{c} \approx 640.$$

Then, at the length of sampling of $f_k/\delta f_k = 10^5$ cycles, a glitch by one cycle occurs and, accordingly, the loss of correlation or misalignment takes place. Therefore, bit streams should be reduced to one clock frequency.

A comparison of signals and the calculation of the delay are performed at the moment t_1 of wave front arrival to the GRT antenna. The SRT position at moment t_2 can be obtained by expanding the power series in terms of τ

$$\mathbf{r}_2(t_2) = \mathbf{r}_2(t_1) + \dot{\mathbf{r}}_2(t_1)\tau + \ddot{\mathbf{r}}_2(t_1)\tau^2 + \ldots. \quad (2)$$

As a results of correlation processing one determines the group delay τ_r and interference frequency f_{int} that are connected with phase φ of interference response by the following relations:

$$\tau_r = d\varphi/d\omega_0, \quad f_{\text{int}} = d\varphi/dt, \quad (3)$$

where $\omega_0 = 2\pi f_0$ is the cyclic frequency of a signal observed by the SRT. The group delay $\tau_r = \tau + \Delta\tau$ includes both geometric signal delay τ and additional signal delay $\Delta\tau$, which depends on other factors, such as gravitational delay, delay in the ionosphere and troposphere, instrumental delay, and clock skew at recording points (TS and GRT). The additional delay $\Delta\tau$ also should be compensated for.

The system of navigation support provides data for calculating the current values of geometric delay τ and interference frequency f_{int}; therefore, when formulating requirements for navigation support, it is necessary to consider only the geometric part τ of the delay τ_r and interference frequency f_{int}.

Let us expand the phase of interference response into a power series in terms of t as follows:

$$\varphi(t) = \omega_0 \frac{V}{c} t + \omega_0 \frac{W}{2c} t^2 + \ldots. \quad (4)$$

One can see from this formula that phase incursion depends not only on velocity, but also on the acceleration of the relative motion of the telescopes. The relationship $(W/c)\pi f_0 t_{\varphi}^2 \leq \Delta\varphi$ should be valid, where $\Delta\varphi$ is incursion (precision of retention) of phase ≈ 0.1 radian. This determines the maximum time of the coherent accumulation of signals.

The interval $\pm\Delta\tau$ of indeterminacy of quantity τ determines the number of necessary exhaustive searches when calculating the correlation function of two bit streams $\xi_1(t)$ and $\xi_2(t)$ as follows:

$$R(\tau) = \int_{-\infty}^{+\infty} \xi_1(t)\xi_2(t+\tau)dt. \quad (5)$$

This determines the number of parallel channels of the correlator. Here, one should also add the error in time synchronization (reference time) of two streams. If the number of parallel channels of digital correlator is sufficient, one can determine the maximum of cross-correlation function and corresponding values of delay τ with an accuracy to one clock cycle duration, i.e., $1/f_k$. Upon finding the maximum value of the cross-correlation function, the refined values of τ_r and f_{int} are determined, which can be used to upgrade and check the predicted position and velocity of SRT.

The bit stream formed by the SRT is transmitted to the TS, where it is referenced to local UTC time. However, the 15-GHz monochromatic signal modulated by this stream is also accompanied by phase changes due to delays in the ionosphere, troposphere, hardware, as well as due to the Doppler and gravitational shifts of frequency. For the precise reference of SRT data, one should take all of these effects into account and compensate for them.

It can be seen from formulas (1)–(5) that, at correlation processing, it is necessary to compensate for the phase difference and its first and second derivatives, which depend above all on errors in determining SRT coordinates, velocity, and acceleration. This fact makes the following demands to the accuracy of the determination of spacecraft motion parameters: at position $\Delta r = \pm 600$ m; at velocity $\Delta V = \pm 2$ cm/s; and at acceleration $\Delta w = \pm 10^{-8}$ m/s^2.

PROBLEMS OF NAVIGATION SUPPORT OF THE MISSION

Methods of orbit determination using the tracking data were developed as early as in the beginning of the 1960s and are currently still in use. Certain updates to these methods are due to new capabilities of modern technical means of observation and computer technology, along with the well-timed delivery of necessary service data, including the data of the systems of global space navigation GPS and GLONASS, parameters of the Earth's rotation, conditions in the ionosphere and troposphere, etc.

The *Spektr-R* spacecraft is a key element of the mission. It has a number of peculiarities that cannot be ignored when one calculates its motion. In the first place, operation of the attitude control and stabilization system represents such a peculiarity, since it causes perturbations of motion of the spacecraft's center of mass. The spacecraft is designed based on the *Navigator* spacecraft bus developed by the Lavochkin NPO as a platform for space observatories. The system of attitude control and stabilization is a part of this module, and it is realized using reaction wheels electromechanical executive devices (EMED) control, which can compensate for external perturbing torques and change spatial orientation of the spacecraft. During the flight the velocity of the EMED reaction wheels can reach such magnitudes that subsequent spacecraft attitude control becomes ineffective or impossible. Because of this, there is need to unload the system, i.e., one must reduce the angular velocity of flywheels substantially and to decrease the spacecraft's angular momentum using stabilization thrusters (ST). The position of ST with respect to the spacecraft body does not allow one to unload flywheels without perturbing motion of the center of mass. On average, the increment of the spacecraft velocity due to an unloading is 3–7 mm/s, and unloadings occur more frequently than once per day. Since the density of performing tracking observations does not allow one to always determine the spacecraft orbit on short arcs between unloadings of reaction wheels, the motion should be reconstructed using long measuring arcs and perturbations due to unloadings must be properly taken into account in the model of motion.

The attitude of the *Spektr-R* spacecraft relative to the Sun changes over time; therefore, for the adequate description of perturbations caused by solar radiation pressure, it is necessary to have a model that takes into account the shape of the spacecraft and its surface properties. Due to the SRT parabolic antenna, the ratio of the cross section area of the spacecraft to its mass can reach a value of 0.03 m^2/kg, and the perturbation produced by solar radiation pressure forces can differ from gravitational perturbations by only one to two orders of magnitude. Thus, an adequate model of solar radiation pressure is a necessary condition for the high-quality reconstruction of the spacecraft orbit on long time intervals.

The motion of a spacecraft with these peculiarities cannot be described well enough by a standard set of orbital parameters, such as orbit elements or the state vector. This set should be supplemented by solar radiation pressure parameters and by parameters characterizing EMED unloadings. In this case, telemetry transmitted to the Earth that contains information about the operation of onboard systems can be used to estimate the unknown parameters of motion along with the main source of data (tracking data).

MODEL OF MOTION

Standard flight of the *Spektr-R* spacecraft proceeds along a passive trajectory interrupted by sessions of unloading EMED accompanied by firings of stabilization thrusters. Unloadings are performed several times a day and represent alternating firings of stabilization thrusters with a goal to damp the total angular momentum of the spacecraft together with reaction wheels. The process takes 1–3 min, during which time several dozen firings of the thrusters occur. Since the spacecraft orbital period exceeds the duration of unloading by many times, the accepted model takes into account the unloading effect on the spacecraft motion as an instantaneous increment of velocity at a weighted average time moment. The increment of spacecraft velocity as a result of a single firing of ST can be calculated using telemetry data containing spacecraft attitude, the duration of the firing, and the mass of the spent propellant. The attitude of the spacecraft determines the increment direction, while the duration of the firing and the mass of propellant identify the thrust and the value of the velocity increment. For a regular session of unloading with index i, the velocity increment vector is designated as $\Delta\mathbf{v}_i$. The time moment t_i when it is applied and the corresponding observed value are determined by the formulas

$$t_i = \left(\sum_{j=1}^{N} \Delta v_{i,j} t_{i,j}\right) \Bigg/ \left(\sum_{j=1}^{N} \Delta v_{i,j}\right), \quad \Delta v_i^0 = \sum_{j=1}^{N} \Delta v_{i,j}, \quad (6)$$

where $t_{i,j}$ is the time of the jth firing of a thruster in the ith session of unloading, $\mathbf{v}_{i,j}$ is the vector of spacecraft velocity increment after the jth activation of ST in the ith unloading derived with the use of telemetric data.

On passive segments of a trajectory the following factors influencing the spacecraft motion are taken into account: the Earth's gravity including the central and non-central parts of the geopotential; gravitation of the Moon, Sun, and planets; variations of gravitational field due to deformation of the Earth under the action of attraction of the Moon and the Sun (solid tides); direct solar radiation pressure; pressure of the Earth's radiation; atmosphere (at segments below 1500 km above the Earth's surface); and additional

perturbing acceleration caused by the general relativity effects.

The gravitational field of the Earth is represented as an expansion in terms of spherical functions of the geopotential in accordance with the EGM-96 model up to the 75 × 75 harmonic [3]. In order to obtain coordinates of the Moon, Sun, and planets, the tables of the motion of the Moon and planets based on theory DE421 [4] are used. To describe the influence of tidal forces, a model is used that takes into account the deformation of the Earth in the direction of a perturbing body (the Moon or the Sun) as a first term in the spherical function expansion of the geopotential [5, 6]. The Earth's radiation pressure is taken into account according to [7]; in this case, the Earth's surface is partitioned in 18 × 9 segments with constant albedo coefficients. The atmosphere density is calculated based on a model recommended by the state standard GOST R 25645.166–2004 [8]. The additional perturbing acceleration caused by general relativity effects is calculated in accordance with the formulas presented in [9].

The solar radiation pressure depending on the attitude of the spacecraft and optical properties of its surface, is one of the main sources of errors originating when one determines and predicts the spacecraft motion parameters.

The model accepted in this paper represents the force acting on an illuminated element of the spacecraft body in the form of a linear combination of three vectors as follows [10, 11]:

$$\mathbf{F}_{\text{el}} = (1-\alpha)\mathbf{F}_b + \alpha\mu\mathbf{F}_s + \alpha(1-\mu)\mathbf{F}_d, \qquad (7)$$

where α is the reflection coefficient; μ is the surface reflectivity; and $\mathbf{F}_b$, $\mathbf{F}_s$ and $\mathbf{F}_d$ are the light pressure forces under assumptions that the surface absorbs light completely, reflects light like mirror, and reflects light diffusely, respectively. Diffuse reflection means reflection according to Lambert's cosine law. It is evident that values of α and μ that describe real materials lie in the interval from zero to unity. The values of basic forces into which the light pressure force is decomposed depend only on the geometry of the surface of an element and light flux direction. Thus, knowing coefficients α and μ for every illuminated element of the surface, using this approach, one is able to calculate the total force of solar radiation pressure acting upon the spacecraft. In the case of the *Spektr-R* spacecraft, a simplified model of its surface was used to calculate the forces. This model includes the SRT antenna, spacecraft bus, and solar panels. The light pressure coefficients α_1 and μ_1 are ascribed to the surface of the SRT antenna and spacecraft bus, while coefficients α_2 and μ_2 were used for the surface of solar panels. The use of identical coefficients for the central block and SRT is justified by the fact that illuminated parts of these elements are coated by the same multilayer thermal insulation. Notice that two coefficients for solar panels are in fact unnecessary. The panels are permanently orientated nearly orthogonal to the Sun. This means that, for them, all three basic forces should be directed almost identically, i.e., along the normal to the panel plane, and coefficients α_2 and μ_2 are not independent. In order to avoid ambiguity, we fix the value $\mu_2 = 0$. Thus, perturbation from the light pressure on the surface of *Spektr-R* spacecraft depends on three parameters, i.e., α_1, μ_1, and α_2.

It follows from the above said that the main sources of errors in the suggested model are associated with perturbations from unloadings of reaction wheels and solar radiation pressure. The key parameters that determine these perturbations are the coefficients of solar radiation pressure α_1, μ_1, α_2 and unloading impulses $\{\Delta\mathbf{v}_i(t_i)\}_{i=1}^m$. In order to improve the accuracy of oirbit determination, the parameters of light pressure and unloadings are included into the number of adjustable parameters, and they are determined as a result of the agreement between observed values and their calculated analogs.

TRACKING AND TELEMETRY DATA

Both standard tracking observations and telemetry data recorded by onboard systems then transmitted to the Earth during regular communication sessions are used in order to determine the motion parameters of *Spektr-R*. Tracking data includes radio measurements of slant range and radial velocity, together with laser range data and astrometric observations of spacecraft position on the celestial sphere in the optical range. Telemetry data used in the calculation of motion includes spacecraft attitude with respect to stars, records of ST firings, and operational data of EMED reaction wheels.

Joint information on the operation of ground facilities of the radio and optical wavelengths is presented in Tables 1 and 2. The radio technical systems based on antennas in Ussuriysk and Medvezhyi Ozera that operate in the C-band form a standard tracking system. In addition, these stations are supplied with equipment for receiving signals of the highly informative radio channel (HIRC) that is used to transmit large amounts of data from spacecraft to the Earth. Since the career frequency of HIRC signals is generated using onboard hydrogen frequency standard and, as a consequence, is highly stable, the received signal frequency measured on the ground contains rather precise information about the topocentric velocity of the spacecraft. However, because the frequency is generated and measured at different places, processing of one-way Doppler measurements requires more sophisticated modeling, as is demonstrated in [12]. The main receiver of HIRC signals is the complex RT-22 of Pushchino Radio Astronomical Observatory through which the scientific measurement data are transmitted from SRT to the ground in the real-time mode. The signal frequency measured at Pushchino is also used for one-way measurements of the radial

Table 1. Measuring facilities of the radio wave band

Measuring system	Range	D	$\dot{D}$	$\dot{D}_{1w}$
Ussuriysk RT-70, CMS Klyon-D	C	+	+	
Ussuriysk RT-70, GBRC Phobos	X			+
Medvezhyi Ozera RT-64, GBCC Cobalt-M	C	+	+	
Medvezhyi Ozera RT-64, Cortex	X			+
Pushchino, RT-22	X, Ku			+
Green Bank, 140-ft	X, Ku			+

Table 2. Measurements by optical facilities from July 18, 2011 to October 1, 2013

Observatory	Aperture, m	Number of trackings	Number of measurements
Caucasus (Chapaly)	1.3	10	4798
Grasse (OCA)	1.54	10	365
Kitab Intern. Latitude Station	0.4	180	2586
Nauchny-1 (CrAO)	0.25–2.6	72	5335
Blagoveshchensk Latitude Station	0.25	83	1127
Evpatoria (Nat. Center of Spacecraft Control and Tests)	0.7	43	2132
Krasnodar (Kuban State Univ.)	0.5	138	7163
Mondy (Inst. of Solar-Terr. Phys.)	0.8, 1.6	31	1162
Uzhgorod (Space Res. Lab. of Nat. Univ.)	0.25	36	864
Mil'kovo	0.22	3	104
Kislovodsk	0.25, 0.4	3	58
Ussuriysk	0.25	2	19
Terskol (Inst. of Astronomy, Rus. Acad. Sci.)	2.0	2	57
Lesosibirsk	0.22	1	3
Zvenigorod (Inst. of Astronomy, Rus. Acad. Sci.)	0.5	1	14
New Mexico (MPC:H15)	0.4	3	31
New Mexico (MPC:H06)	0.1	53	1450
Australia (MPC:Q62)	0.32	12	144

Observatories at Caucasus and in Grasse make laser measurements of inclined range, while all other observatories make angular measurements of spacecraft's right ascension and declination.

velocity. Starting from autumn of 2013, the NRAO complex at Green Bank with an antenna diameter of 42 m also performs one-way Doppler measurements and receives scientific data from the spacecraft that supplement those of Pushchino observatory.

Due to their high precision, laser measurements are among the most informative sources of orbital information. However, in the case of *Spektr-R* spacecraft, these measurements are connected with some difficulties. Since the array of retroreflectors is fixed with respect to the body of the spacecraft, to carry out measurements, it is necessary to have a certain spacecraft attitude in space. In addition, only a few observatories are capable of operating at distances of spacecraft flight, and the successful implementation of measurement sessions strongly depends on the weather conditions. The Russian laser optical locator at the Caucasus and French observatory OCA in Grasse succeeded in carrying out laser measurements for the distance to the *Spektr-R* spacecraft as a part of a collaboration with the ILRS international network of laser tracking.

Most astrometric optical measurements are performed by participants of the International Scientific Optical Network (ISON) and by facilities engaged by the Astro Space Center of the Lebedev Physical Insti-

tute. This type of measurement has rather modest accuracy when converted to Cartesian coordinates compared to traditional radio technical distance measurements. However, it yields an estimate of direction, i.e., the spacecraft position in the plane orthogonal to the radial direction. This estimate can also be derived from radial measurements accumulated over a time interval using the spacecraft dynamics. Nevertheless, for spacecraft whose motion proceeds far from attracting bodies, the efficiency of the results of this approach is low, since, due to weak dynamics, one must use long measurement intervals on which the errors in the motion model become substantial. Astrometric measurements allow one to obtain more precise orbits in short intervals; they also help to exercise control over the quality of orbits obtained with long measurement arcs.

To model the spacecraft dynamics, the key type of telemetry data is spacecraft attitude with respect to the inertial frame. Solar radiation pressure forces depend on the attitude, as well as the direction, of unloading impulses, since STs are fixed relative to the body of the spacecraft. During a flight, the data of star sensors are sampled, processed onboard the spacecraft, and written to the telemetry data stream at a rate of one every few minutes. Attitude at an arbitrary time moment is calculated with the help of a uniform (in time) rotation between two adjacent points from telemetry with well-known orientation.

According to Eq. (6), the measurement of unloading impulse $\Delta\mathbf{v}_i^0$ can be derived from measurements of velocity increment $\Delta\mathbf{v}_{i,j}$ at separate firings which in turn depend on telemetry data in the following way:

$$\Delta v_{i,j} = (1/M)\Delta m_{i,j} I_y(\tau_{i,j}) g \mathbf{e}_{i,j}, \tag{8}$$

where M is current mass of the spacecraft; $\Delta m_{i,j}$ is the mass of the spent propellant; I_y is the thruster's specific thrust and the known function of the duration of the firing $\tau_{i,j}$; g is the free fall acceleration; and $\mathbf{e}_{i,j}$ is the known direction of thruster thrust. The measured value includes errors in the magnitude determined by measured values of $\Delta m_{i,j}$ and $\tau_{i,j}$, as well as in direction $\mathbf{e}_{i,j}$. These errors are connected with the errors of attitude determination during unloading and errors in determining the direction of thrust in the spacecraft-fixed coordinate system. The a priori estimation of the error of determining $\mathbf{e}_{i,j}$ is equal to 1°, i.e., the orthogonal component of the error in determining the velocity increment is small, and quantity $\Delta\mathbf{v}_{i,j}$ can be considered a normal vector with the covariance matrix

$$\mathbf{K} = \sigma_d^2(\mathbf{E} - \mathbf{e}\cdot\mathbf{e}^{\mathrm{T}}) + \sigma_v^2 \mathbf{e}\cdot\mathbf{e}^{\mathrm{T}}, \tag{9}$$

Here, $\mathbf{e} = \mathbf{e}_{i,j}$ is the velocity increment direction, σ_v is the error of magnitude determination, and σ_d is the error in the orthogonal direction. In calculations, the orthogonal error was specified in accordance with the angular error as 1°, and the error of quantity was calculated in such a way that it would be in correspondence with errors of execution for stabilization thrusters equal to 10%.

From the point of view of information about spacecraft motion parameters the data on EMED operation (namely, on the rotation speed of reaction wheels) are useful. In the general case, knowledge of parameters of the rotation of the spacecraft as a whole around its center of mass and knowledge of how its reaction wheels rotate allow one to estimate the torque due to external forces acting upon the spacecraft. For about 90% of the time, the *Spektr-R* spacecraft is located at distances from the Earth exceeding 100000 km, where the average torque produced by the solar radiation pressure is larger by two orders of magnitude than the maximum possible gravitational torque. For a majority of the time, the spacecraft keeps an invariable attitude, i.e., the total angular momentum of the spacecraft only changes due to reaction wheels. Let us consider time interval (t_1, t_2), which is several hours long, during which the spacecraft is at a distance of greater than 100000 km from the Earth, and its attitude is invariable with respect to stars. Over this time, the Sun's orientation changes insignificantly with respect to the spacecraft, as well as distance to the Sun, and the following expression is valid:

$$\sum_{j=1}^{M} \mathbf{a}_j I_j(\Omega_j(t_2) - \Omega_j(t_1)) = \mathbf{M}_{sp}(\alpha_1, \mu_1, \alpha_2, \mathbf{r}, \Lambda)(t_2 - t_1), \tag{10}$$

where summation on the left-hand side is made over spacecraft reaction wheels, $\mathbf{a}_j$ are direction cosines of the flywheel rotation axis, I_j is the inertia moment of a flywheel about its axis of rotation, $\Omega_j(t)$ is the angular velocity of flywheel rotation measured by the onboard system, $\mathbf{M}_{sp}$ is the torque due to solar radioaton pressure forces, $\mathbf{r}$ is the spacecraft's radius vector, and Λ is the attitude quaternion of the spacecraft. The dependence of the solar radiation torque on light pressure coefficients coincides with the structure of expression (7) for the light pressure force. The left-hand side of (10) depends on measured quantities $\Omega_j(t)$, while the right-hand side includes unknown coefficients of light pressure.

Let us introduce the following discrepancy:

$$\xi = \frac{\sum_{j=1}^{M} \mathbf{a}_j I_j(\Omega_j(t_2) - \Omega_j(t_1))}{t_2 - t_1} - \mathbf{M}_{sp}(\alpha_1, \mu_1, \alpha_2, \mathbf{r}, \Lambda), \tag{11}$$

which describes the difference of oserved and calculated torques of solar radiation pressure forces, which can be used on orbit determination. Figure 2 presents the time dependences (reconstructed from telemetry data) of velocities $\Omega_j(t)$ and reaction wheels' angular momentum $\mathbf{K}(t) = \sum_{j=1}^{M} \mathbf{a}_j I_j \Omega_j(t)$ in the bound coordinate system on the interval February 22–23, 2013. The

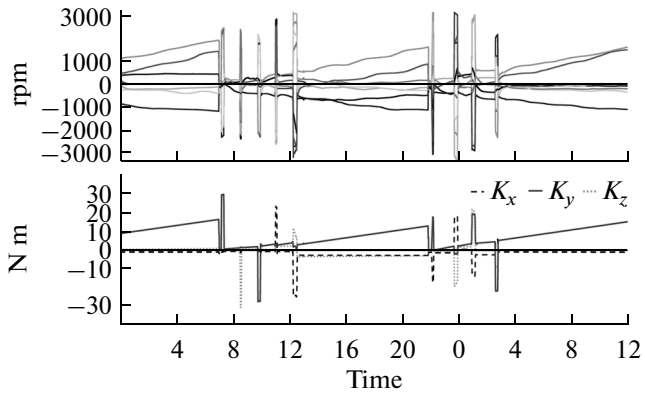

Fig. 2. Changing parameters of EMED as recorded by telemetry.

spikes of velocities of reaction wheels' rotation in the plot correspond to changes in spacecraft attitude and, for the rest of the time, the attitude was kept invariable in the inertial frame. Real data confirm that the torque of external forces is constant in intervals with fixed attitude, while the angular momentum of reaction wheels increases linearly. The rate of variation in the angular momentum changes together with orientation because of the changing moment of solar radiation pressure forces.

ORBIT DETERMINATION

Let us consider the motion of the spacecraft on the time interval $[t_{\text{in}}, t_{\text{f}}]$. We assume that n unloadings of reaction wheels occurred during this interval. From telemetry, we know times and observed values of unloading impulses

$$(t_1, \Delta\mathbf{v}_1^0), (t_2, \Delta\mathbf{v}_2^0), \ldots, (t_n, \Delta\mathbf{v}_n^0), \quad t_i \in [t_{\text{in}}, t_{\text{f}}], \quad i = 1, \ldots, n. \tag{12}$$

The light pressure is described by a set of three parameters, i.e., α_1, μ_1, and α_2. Let trajectory measurements $\mathbf{\Psi}_0$ be made on the specified time interval. In the general case, they include measurements of slant range, radial velocity, and angular position of the spacecraft. Suppose that, over time, in the interval under consideration, the spacecraft was in an invariable attitude a number of N times. For each of these events, we determine the timetable (t_1^j, t_2^j) and values of discrepancies obtained from (11). Let us specify the following extended vector of parameters that determine the spacecraft motion as follows: $\mathbf{Q} = \{\mathbf{X}_0(t_0), \alpha_1, \mu_1, \alpha_2, \Delta\mathbf{v}_1, \ldots, \Delta\mathbf{v}_n\}$, where $\mathbf{X}_0(t_0)$ is the spacecraft's state vector for the moment $t_0 \in [t_{\text{in}}, t_{\text{f}}]$. We use the coordinates and velocity of the spacecraft in the inertial space as a state vector. Using the introduced designations, let us define the following functional:

$$\Phi = (\mathbf{\Psi}_0 - \mathbf{\Psi}_c)^{\mathrm{T}} \mathbf{P} (\mathbf{\Psi}_0 - \mathbf{\Psi}_c) + \sum_{j=1}^{N} \xi_j^{\mathrm{T}} \mathbf{P}_j^{sp} \xi_j + \sum_{i=1}^{n} (\Delta\mathbf{v}_i^0 - \Delta\mathbf{v}_i)^{\mathrm{T}} \mathbf{P}_i (\Delta\mathbf{v}_i^0 - \Delta\mathbf{v}_i), \tag{13}$$

where $\mathbf{\Psi}_0$ is the observed (measured) values of trajectory measurements, $\mathbf{\Psi}_c$ is calculated values of trajectory measurements depending on the spacecraft motion $\mathbf{\Psi}_c = \mathbf{\Psi}_c(\mathbf{Q})$, $\mathbf{P}$ is the weight matrix of trajectory measurements, $\mathbf{P}_j^{sp}$ is the weight matrix of light pressure moments, and $\mathbf{P}_i$ is the weight matrix of measurements of impulses obtained from the sum of covariance matrices of separate switches (9) of unloadings. Expression (13) differs from the functional used in the classic variant of orbit determination according to trajectory measurements by the maximum likelihood method [13]; here, there are two additional terms. Each of these terms includes a mismatch between functions of measured values provided by the telemetry system and calculated values depending on elements $\mathbf{Q}$. In this sense, their separation from trajectory measurements is conventional. We assume that the mismatch errors of both trajectory measurements and measurements of unloading impulses and light pressure moments are distributed normally with zero mathematical expectations.

We will seek the motion parameters $\mathbf{Q}^*$ that deliver a maximum to the likelihood function $L(\mathbf{\Psi}|\mathbf{Q}) = P(\mathbf{Q}|\mathbf{\Psi})$, which is (for the normal distribution) equivalent to $\mathbf{Q}^* = \min\arg\Phi(\mathbf{Q})$.

The search for unknown values of $\mathbf{Q}^*$ is performed by the same methods as in the case of only trajectory measurements available. In particular, the parameters can be found by the iteration method of generalized Newton tangents using, e.g., the solution obtained by refining only state vector $\mathbf{Q} = \mathbf{X}_0(t_0)$ as the initial approximation.

RESULTS

Let us estimate the influence of the above models and methods on the quality of the *Spektr-R* orbit obtained as a result of adjustment, where the real trajectory measurements and telemetry data are the input data for obtaining the orbit.

Two time intervals of 2013 were selected in order to determine the orbit, i.e., from February 20 to April 10 and from April 10 to May 30. On one hand, the selected intervals are in the zone of intense observations and, on the other hand they are at the maximum distance from the moment of injection into orbit in order to avoid errors connected with adjustment of new measurements systems.

Table 3. Dimensionless orbit quality of trajectory measurements

Model	Light pressure	Unloadings	σ_1, 20 Feb–10 Apr, 2013	σ_2, 10 Apr–30 May, 2013
"K"	Classical, χ	Not taken into account	12.43677	9.18588
"KP"	Classical, χ	Taken into account	4.72914	6.78832
"CP"	Complex, α_1, μ_1, α_2	Taken into account	1.20896	0.63767
"CP+"	Complex, α_1, μ_1, α_2	Solved for	0.36210	0.31607

The model of motion described above, including the model of solar radiation pressure depending on three adjustable parameters α_1, μ_1, α_2 and adjustable impulses of unloadings of reaction wheels, will be used as a basic model for reconstructing the spacecraft orbit in the selected time intervals. In order to estimate the manner in which allowance for functional and construction properties of the spacecraft influences the quality of resulting orbit, let us consider three additional models.

The first model of motion is classical and takes into account all external perturbations of passive motion described above, excluding the solar radiation pressure, which is described by a simple model [14] that is valid for a uniformly colored sphere. In this paper, the following realization of the simple model of acceleration produced by light pressure was used:

$$\mathbf{a}_{sp} = -\chi \frac{\mu_S}{|\mathbf{R}_S - \mathbf{r}|^3}(\mathbf{R}_S - \mathbf{r}),$$

where μ_S is the gravitational parameter of the Sun, $\mathbf{R}_S$ is the radius vector of the Sun, and $\mathbf{r}$ is the spacecraft's radius vector. In this case, the solar radiation pressure does not depend at all on spacecraft attitude and is characterized by a single coefficient χ that is included in adjustable parameters.

The second model describes the classical passive motion but with added reaction wheels unloadings. The solar radiation pressure is also described by a single coefficient that is solved for. Unloading impulses have fixed values that coincide with those measured (obtained from telemetry).

The third model, like the second one, uses measured values of unloading impulses without adjusting them. The light pressure is described by three coefficients α_1, μ_1, and α_2, which are adjusted together with the initial state vector.

The results of matching the measurements on different time intervals obtained after convergence of the orbit determination process are presented in Table 3. Dimensionless root-mean-square deviation $\sigma = \sqrt{\Phi/N_{\text{meas}}}$ is chosen as a quantity that characterizes the matching of measurements. When determing the orbit, constant values of root-mean-square errors of measurements were used, as well as the values of weights and weight matrices that correspond to them. The error of distance measurement was assumed to be equal to 100 m. The error of measuring the radial distance was specified at levels of 10 and 5 mm/s for two-way and one-way measurements, respectively. It was also assumed that errors of measuring right ascension and declination were equal to 1 arcsec and had no correlation between themselves. It should be noted that, when calculating σ for CP+ model only a part of the functional (corresponding to trajectory measurements) was used. Measurements' ageement by applying the CP+ model, which is most sophisticated, is illustrated in Figs. 3–5 and 7–9. In both intervals, the matching of measurements is better than a priori values of the errors taken for weights of measurements. With the exception of sporadic outliers, the trajectory measurements of distance taken in Ussuriysk lie within a design accuracy of 20 m for both intervals. The matching of measurements made in Medvezhyi Ozera is a bit poorer; however, most of them lie within 50 m. Systematic deviations in the radial velocity do not exceed 2 mm/s. Optical measurements agree with the obtained orbit to an accuracy better than 1 arcsec.

Figures 6 and 10 present discrepancies between observed and calculated values of unloading impulses together with deviations of the directions of calculated impulses. The root-mean-square errors of determining the values of unloading impulses were equal to

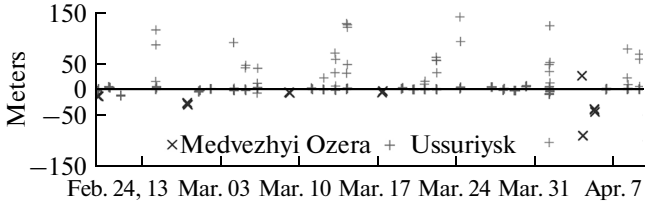

Fig. 3. CP+ Model and distance residuals for February 20, 2013–April 10, 2013.

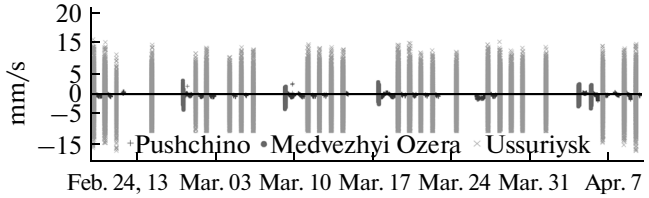

Fig. 4. CP+ Model and radial velocity residuals for February 20, 2013–April 10, 2013.

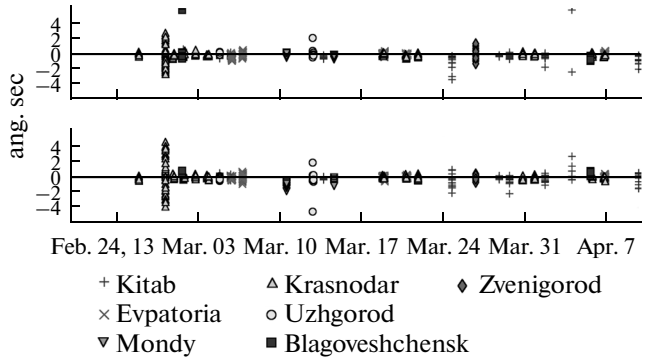

Fig. 5. CP+ Model and direction residuals for February 20, 2013–April 10, 2013.

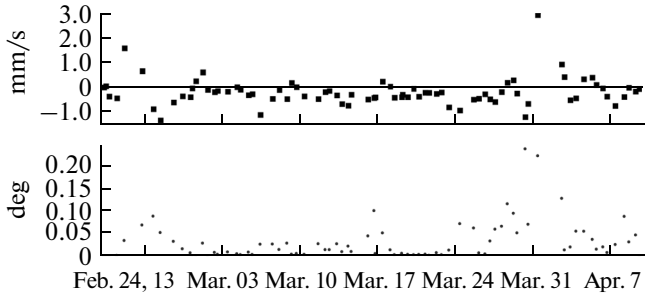

Fig. 6. CP+ Model and unloading impulse residuals for February 20, 2013–April 10, 2013.

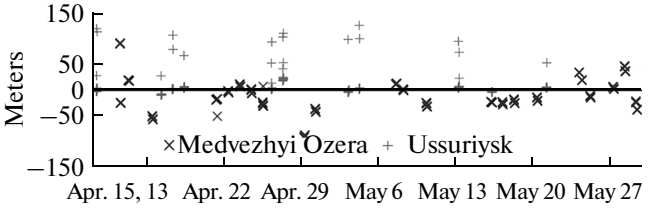

Fig. 7. CP+ Model and distance residuals for April 10, 2013–May 30, 2013.

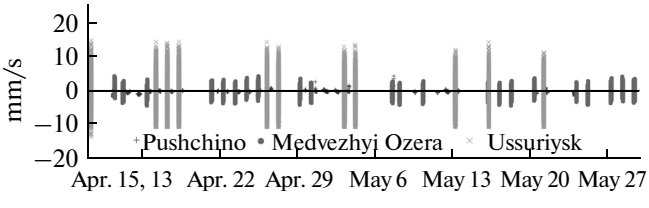

Fig. 8. CP+ Model and radial velocity residuals for April 10, 2013–May 30, 2013.

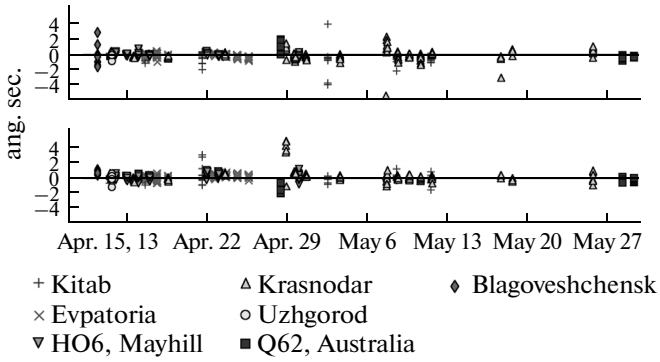

Fig. 9. CP+ Model and direction residuals for April 10, 2013–May 30, 2013.

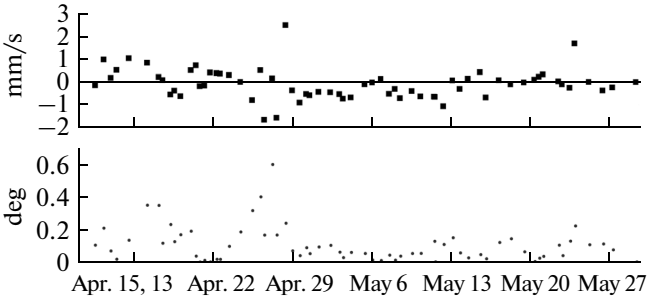

Fig. 10. CP+ Model and unloading impulse residuals for April 10, 2013–May 30, 2013.

0.5928 and 0.6566 mm/s on the first and second intervals, respectively. Angular deviations do not exceed 0.7°.

Tables 4 and 5 present compiled values of motion parameters determined on two measuring intervals and reduced to identical time t_0 corresponding to midnight of universal time between April 9 and 10, 2013. For convenience, the state vectors are represented in osculating elements. One can see from these tables that the coefficients of light pressure derived as a result of using identical models on different measuring intervals are consistent with each other. In this case, the coefficient χ decreases when one passes from the K model to the KP model in both intervals. This is because, in view of the admissible attitude of *Spektr-R* spacecraft, the perturbation produced by reaction wheels unloading will always have a nonzero component in the direction away from the Sun, and the increased coefficient of solar radiation pressure partially takes into account the regular influence of these perturbations. The motion parameters determined by means of the CP+ model agree well with each other on two intervals in both the coordinate sector and the coefficients of light pressure.

The estimates made on two measuring intervals show that the use of sophisticated model of light pres-

Table 4. Parameters of motion refined on the interval February 20–April 10, 2013 and reduced to the moment 00:00:00 UT on April 10, 2013

Parameter	"K"	"KP"	"CP"	"CP+"
a, thous. km	176.814766841	176.814968720	176.815074330	176.815048801
e	0.738340958	0.738333302	0.738330424	0.738329467
i, deg	70.927401302	70.928335431	70.926823804	70.925978782
ω, deg	2.678520144	2.686516018	2.689478581	2.689175151
Ω, deg	291.810779777	291.805612874	291.801806993	291.803042599
M, deg	263.781697920	263.782355379	263.782236339	263.782140582
χ	2.665864×10^{-5}	2.117495×10^{-5}		
α_1			0.79055313	0.85658688
μ_1			0.05319324	0.07669267
α_2			0.00694521	0.10854078

Table 5. Parameters of motion refined on the interval April 10–May 30, 2013 and reduced to the moment 00:00:00 UT on April 10, 2013

Parameter	"K"	"KP"	"CP"	"CP+"
a, thous. km	176.817134121	176.816037584	176.815114242	176.815074736
e	0.738350970	0.738327793	0.738329609	0.738330220
i, deg	70.928685124	70.924122602	70.925521172	70.926031934
ω, deg	2.693601490	2.692458506	2.689089394	2.689208150
Ω, deg	291.808505413	291.807847533	291.803134632	291.803084043
M, deg	263.787776530	263.783246435	263.782256506	263.782273595
χ	2.793778×10^{-5}	2.060516×10^{-5}		
α_1			0.83780732	0.86560409
μ_1			0.07362764	0.13378616
α_2			0.07057908	0.13462086

sure and allowance for perturbations produced by flywheel unloading can improve the matching of measurements by factors of seven and thirteen compared with the classic model of passive motion. The additional refinement of unloading impulses allows one to improve the above values up to factors of 34 and 29, respectively. Equally important is the fact that in CP+ model unloading impulses were adjusted to values similar in direction to the measured ones, and deviations of their values have no significant systematic character, which would be evidence of existing poor modelled perturbations. The suggested model of solar radiation pressure adequately describes perturbations of the motion of the spacecraft's center of mass. The estimated values of coefficients α_1, μ_1, and α_2 support this, since they lie in the region of admissible values and are located rather close to each other when refined in different intervals. In addition, the coefficient values correspond to the surfaces to which they were attributed. The antenna and central unit are coated by multilayer insulation, which reflects light well, while solar array panels, as could be expected, absorb a majority of the incident light.

ACKNOWLEDGMENTS

The RadioAstron project is being carried out by the Astro Space Center of Lebedev Physical Institute and by the Lavochkin NPO under contract with the Rus-

sian Space Agency, along with numerous scientific and engineering institutions of Russia and other countries.

REFERENCES

1. Kardashev, N.S., Pariiskii, Yu.N., and Sokolov, A.G., Space radio astronomy, *Usp. Fiz. Nauk*, 1971, vol. 104, no. 6, pp. 328–331.
2. Andreyanov, V.V. and Kardashev, N.S., Project of a ground–space interferometer, *Kosm. Issled.*, 1981, vol. 19, no. 5, pp. 763–772. {*Cosmic Research*, p. 527].
3. Lemoine, F.G., Kenyon, S.C., Factor, J.K., et al., *The Development of the Joint NASA GSFC and National Imagery and Mapping Agency (NIMA) Geopotential Model EGM96*, NASA/TP-1998-206861, Greenbelt, Maryland: Goddard Space Flight Center, 1998. http://www.nima.mil/GandG/wgs-84/egm96.html
4. Folkner, W.M., Williams, J.G., and Boggs, D.H., The planetary and lunar ephemeris DE421, *Interplanetary Network Progress Report*, August 2009, vol. C1, pp. 42–178.
5. Eanes, R.J., Shtutz, B., and Tapley, B., Earth and ocean tide effects on *Lageos* and *Starlette*, *Sckweizerbartsche Verlagabuchhandlung*, October 1983, p. 239–250.
6. Mathews, P.M., Herring, T.A., and Buffet, B.A., Modeling of nutation–precession: New nutation series for nonrigid Earth, and insights into the Earth's interior, *J. Geophys. Res.: Solid Earth*, 2002, vol. 107, no. B4, pp. 1–27.
7. Knocke, P.C., Ries, J.C., and Tapley, B.D., *Earth Radiation Pressure Effects on Satellites*, American Institute of Aeronautics, Astronautics, 1988.
8. *GOST* (State Standard) *R 25645.166–2004: Upper Atmosphere of the Earth: A Model of Density for Ballistic Support of Flights of the Earth's Artificial Satellites*, Fedorova, R.S., Ed., TsNII Minoborony Rossii, 2004.
9. Estabrook, F.B., Post-Newtonian *n*-body equations of the Brans–Dicke theory, *Astrophys. J.*, 1969, vol. 158, pp. 81–83.
10. Fliegel, H.F., Gallini, T.E., and Swift, E.R., Global positioning system radiation force model for geodetic applications, *J. Geophys. Res.*, 1992, vol. 92, no. B1, pp. 559–568.
11. Komarov, M.M., Sazonov, V.V., and Klimovich, D.N., Calculation of forces and moments of the light pressure acting on a rotor solar sail, *Preprint of Keldysh Inst. of Applied Math., Russ. Acad. Sci.*, 1995, no. 59.
12. Sazhin, M.V., Vlasov, M.V., Sazhina, O.S., and Turyshev, V.G., RadioAstron: Relativistic change of frequency and a shift of the time scale, *Astron. Zh.*, 2010, vol. 87, no. 11, pp. 1–16.
13. Akim, E.L. and Eneev, T.M., Determination of motion parameters for a spacecraft using the data of tracking measurements, *Kosm. Issled.*, 1963, vol. 1, no. 1, pp. 5–50.
14. Abalakin, V.K., Aksenov, E.P., Grebenikov, E.A., Demin, V.G., and Ryabov, Yu.A., *Handbook on Celestial Mechanics and Astrodynamics*, Moscow: Nauka, 1976.

Translated by A. Lidvansky